Sedimentation of active colloidal suspensions

Jérémie Palacci, Cécile Cottin-Bizonne, Christophe Ybert, and Lydéric Bocquet
LPMCN; Université de Lyon; Université Lyon 1 and CNRS,
UMR 5586; F-69622 Villeurbanne, France

In this paper, we investigate experimentally the non-equilibrium steady state of an active colloidal suspension under gravity field. The active particles are made of chemically powered colloids, showing self propulsion in the presence of an added fuel, here hydrogen peroxide. The active suspension is studied in a dedicated microfluidic device, made of permeable gel microstructures. Both the microdynamics of individual colloids and the global stationary state of the suspension under gravity – density profiles, number fluctuations – are measured with optical microscopy. This allows to connect the sedimentation length to the individual self-propelled dynamics, suggesting that in the present dilute regime the active colloids behave as 'hot' particles. Our work is a first step in the experimental exploration of the out-of-equilibrium properties of artificial active systems.

PACS numbers:

The collective behavior of 'active fluids', made of self-propelled entities, has raised considerable interest over the recent years in the context of non-equilibrium statistical physics [1–8]. Such systems are rather common in living systems, from swimming cells, bacteria colonies [9–13], to flocks of birds or fishes [2]. These entities move actively by consuming energy and their behavior is thus intrinsically out of equilibrium. Building a general framework describing their collective properties remains accordingly a challenging task and led to a considerable amount of work towards this aim [1–8]. By contrast, much less work has been performed on the experimental side, and mainly on assemblies of living micro-organisms – which are naturally self-propelled – [11–14], however at the expense of a lack of control and flexibility of the individual particles and their interactions. There is therefore a need for new experiments based on *artificial* model systems, involving suspensions of microscopic active particles with controled propulsion and interaction mechanisms – here designated as '*active suspensions*'. Several routes to design individual artificial microscopic swimmers have been explored recently [15–17], taking benefit of the recent progress made to shape and design colloidal particles at microscales. However going from the individual to the many particles situation remains a challenging task and has not been achieved up to now with artificial motile particles.

In this paper we explore experimentally the behavior of a dilute active suspension of articial swimmers under an external (gravity) field. This problem was discussed theoretically in a recent contribution by Tailleur and Cates [8]. Here the active colloids are powered chemically, following the route proposed by Howse *et al.* [15]. The asymetric dismutation of hydrogen peroxide (H_2O_2) on the colloid itself is used as the driving power, on the basis of a self (diffusio-) phoretic motion, induced by the building up of an osmotic pressure gradient at the interface of the colloid [18–20]. Furthermore a specifically designed microfluidic system based on a gel-microdevice technology has been developed, allowing to ensure constant renewal of the chemical *fuel* (H_2O_2), as well as removal of *waste* products (O_2), in an open reactor configuration. On the basis of this device, we have explored the behavior of the active suspensions at two complementary levels: we have first characterized the individual dynamics of active colloids by particle tracking measurements; then we have investigated the behavior of a dilute active suspension of these particles under an external gravity force field, in the same spirit as the historical Jean Perrin experiment [21]. This allowed us to connect the micro-dynamics of

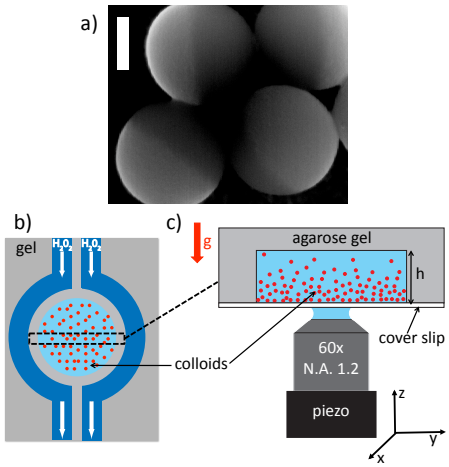

FIG. 1: (a) SEM picture of janus, platinum-latex, colloids (scale bar 500nm). (b) Sketch of the experimental setup: a circular microfluidic chamber (diameter $\Phi = 650\mu$m, height $h \sim 80\mu$m) molded in agarose gel (gray areas) contains the 1μm janus colloids. H_2O_2 feeding is achieved by constant circulation (40μL/min flow rate) in side channels (dark blue). (c) The active colloidal suspension is observed through a piezo-driven high numerical aperture objective (Nikon, Water immersion 60×, NA=1.2) mounted on an inverted microscope.

individual entities to the macroscopic equilibrium behavior of the suspension, allowing to probe the link between fluctuations and dissipation in this configuration.

Active colloids and experimental setup – A monolayer of commercial fluorescent latex colloids (1 μm diameter, Molecular Probes F8823) is formed on a silicon wafer by evaporation from 10^3 dilution in isopropanol (99.99%, Roth), and coated with 2nm platinum by sputtering, see Fig-1-a. Resuspension is achieved by sonication in ultra-pure water (Milli-Q, resistivity 18.2 MOhm.cm^{-1}), leading, after centrifugation, to 50 μL of a janus colloidal solution at $\sim 0.1\%$ v/v (about 10^9 particles/mL). Such janus particles were shown to self-propel in a solution of hydrogen peroxide, due to the dismutation of this chemical on the platinum covering half of the colloids [15]. The properties of this colloidal suspension are then investigated in a dedicated microfluidic device, sketched in Fig.1-b-c. It is made of a circular microfluidic chamber (diameter $\Phi = 650\mu$m, height$\simeq 80\mu$m, volume $V \simeq 30n$L) molded in agarose gel [22, 23], and surrounded by two side channels separated by 125μm gel walls. The central chamber is initially filled with janus colloids, while H_2O_2 solution at concentration C_0 is continuously circulated in lateral channels. This gel microsystem ensures a constant renewal of H_2O_2 fuel and removal of chemical waste products (O_2) by diffusion through hydrogel walls from the infinite reservoir and sink constitued by the circulating lateral channel. This provides a convection-free environnement in the colloids chamber with stable chemical conditions over hours, allowing to study solutions of active colloids (while a similar study would be precluded in a capillary due to the production of oxygen bubbles). In this configuration we then performed measurements of both the dynamics of the colloids and their sedimentation properties, for various concentrations C_0 of the fuel.

Colloid micro-dynamics – First, the dynamics of individual active colloids is investigated using high speed tracking measurements to resolve temporally the different dynamical regimes (see below). For various H_2O_2 concentrations C_0, the two-dimensional (x,y) motion of colloids is recorded with a high speed camera (Phantom V5) at 100Hz and trajectories are extracted with a single particle tracking algorithm (Spot Tracker, Image J [24]). The mean square displacement of the colloids is obtained as $\Delta L^2(\Delta t) = \langle(\vec{R}(t+\Delta t) - \vec{R}(t))^2\rangle$ where $\vec{R}(t)$ is the (2D) instantaneous colloid position and the average is performed over time for each individual trajectory and then over an ensemble of trajectories (typically 20). We plot in Fig. 2 $\Delta L^2(t)$ as a function of time for bare (non-active) and active colloids in a solution of hydrogen peroxide, confirming the impact of injected chemical power on the individual motion of the colloids, in agreement with Ref. [15]. For the bare (non-active) colloids, the dynamics is purely diffusive with a

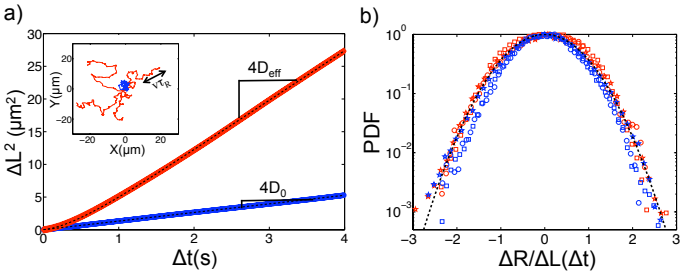

FIG. 2: (a) Experimental mean squared displacements $\Delta L^2(\Delta t)$ and 2D trajectories (inset) for bare (blue) and active colloids (red) in 7.5% H_2O_2 solution. Bare colloids (bottom) show standard diffusion (ΔL^2 linear in time), while the mean squared displacement of active colloids is fitted according to Eq.(1). The measured diffusion coefficients are $D_0 = 0.33\mu\text{m}^2/s$ for bare and $D_{\text{eff}} = 1.9\mu\text{m}^2/s$ for active colloids. (b) PDF of particle displacement ΔR for various lag time Δt as a function of the normalized displacement $\Delta R/\Delta L(\Delta t)$. Δt=0.3s($\star$), 1s($\circ$), 3s($\diamond$) for bare (blue) and active colloids (red) in a solution of 7.5% of H_2O_2. The dashed lines is the gaussian curve.

diffusion coefficient $\Delta L^2/4\Delta t = D_0 = 0.34 \pm 0.02\mu\text{m}^2/s$, which is found to be independent of the H_2O_2 concentration. Note that the same value and behavior is obtained for janus colloids in the absence of the H_2O_2 fuel. For the janus active colloids in a hydrogen peroxide solution, the mean square displacement differs drastically from the equilibrium diffusive dynamics and strongly depends on the fuel concentration. The colloid exhibits ballistic motion at short times, $\Delta L^2(t) \sim V^2t^2$, while at longer times a diffusive regime, $\Delta L^2(t) \sim 4D_{\text{eff}}t$, is recovered with an effective diffusion coefficient D_{eff} much larger than the equilibrium coefficient D_0. As discussed in [7, 15], the active colloids are expected to perform a persistent random walk, due to a competition between ballistic motion under the locomotive power (with a constant swimming velocity V), and angular randomization due to thermal rotational Brownian motion. The transition between the two regimes occurs at the rotational diffusion time τ_r of the colloids. The characteristic ballistic length scale is accordingly $a = V \times \tau_r$. For time scales long compared to τ_r, the active colloids therefore perform a random random walk with an effective diffusion $D_{\text{eff}} = D_0 + V^2\tau_r/4$. The full expression of the mean squared displacement at any time is obtained as [15] :

$$\Delta L^2(\Delta t) = 4D_0\Delta t + \frac{V^2\tau_r^2}{2}\left[\frac{2\Delta t}{\tau_r} + e^{\frac{-2\Delta t}{\tau_r}} - 1\right] \qquad (1)$$

We fit the experimental mean squared displacement $\Delta L^2(\Delta t)$ using Eq. (1) with the propulsion velocity V as the only free parameter, while the value of D_0 is taken from the equilibrium diffusion coefficient measured in water and the Stokes expectation is used for τ_r ($\tau_r = 0.9$s). As shown in Fig. 2-a, an excellent agreement with the experimental results is found. Under the present condi-

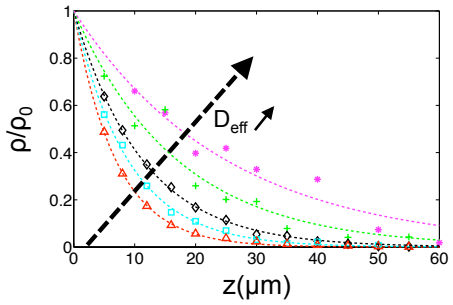

FIG. 3: Normalized density profiles $\rho/\rho_0(z)$ for the active colloidal suspension in stationary state, for increasing swimming activity, *i.e.* increasing $D_{\rm eff}$. Experimental data (symbols) are well fitted by an exponential decay $\rho(z) = \rho_0 \exp(-z/\delta_{\rm eff})$, with a sedimentation length $\delta_{\rm eff}$, which strongly depends on (and increases with) the swimming activity. Here $\delta_{\rm eff}$ varies from 6μm at equilibrium up to 21μm.

tions, the measured propulsion velocities V range from 0.3 $\mu m/s$ to $2.5\mu m/s$, corresponding to an increase of the effective diffusion coefficient by a factor up to 5.5 as compared to the bare diffusion. In the following we use this measure of $D_{\rm eff}$ as a probe of the colloidal 'activity'. Finally we have also measured the probability distribution function (PDF) of the colloid displacement $\Delta R = |\vec{R}(\Delta t) - \vec{R}(0))|$ for a given time lag Δt, see Fig.2-b, both for bare (blue) and active (red) colloid particles. In both cases, the PDF fits very well to a gaussian with variance $\Delta L^2(\Delta t)$ given in Eq. (1). Even though departures from a gaussian are expected at short time for the persistent random walk, these are within experimental uncertainty.

Sedimentation of active particles – We now turn to the investigation of the sedimentation of an assembly of such active colloids, probed in a sedimentation experiment, in the same spirit as the historical Jean Perrin experiment [21]. At thermal equilibrium with a bath at temperature T, a dilute population of colloid with (buoyant) mass m under gravity g exhibits a steady Boltzmann distribution profile $\rho(z) = \rho_0 \exp(-z/\delta_0)$ with $\delta_0 = k_{\rm B}T/mg$ the sedimentation length, which balances gravitational and thermal energy. Alternatively this density profile can be seen as the stationary solution of the Smoluchowsky diffusion-convection equation, $\partial_t \rho + \nabla \cdot J = 0$, with $J = -D_0 \nabla \rho + \mu\, mg\, \rho$ the particle flux, and D_0, μ the colloids diffusion coefficient and mobility. This leads to the fluctuation-dissipation relationship $D = k_{\rm B}T\mu$. In order to explore the validity of these concepts for the out-of-equilibrium active suspension, we have measured – simultaneously to the individual particle tracking experiments – the density profiles $\rho(z)$ of the colloids in the microfluidic chamber, for various fuel concentration C_0. Colloid profiles are measured by scanning the chamber using a piezo-mounted microscope objective (PIFOC P-725.2CD, Physik Instrumente). At each altitude z, a stack of images with lateral dimensions $150 \times 200\mu$m is acquired at 0.3 Hz with a fluorescence camera (Orca, Hamamatsu). On each stack, image analysis is performed with Matlab: first the maximum fluorescence intensity $I_{\rm foc}$ is determined from "in-focus" colloids, then a $0.3 I_{\rm foc}$ threshold criterion is applied in order to discard out-of-focus colloids, thus defining a slice with thickness of $\pm$ 2μm [25]. A stack of 100 images is used to obtain a good statistical convergence. Overall this allows to obtain the average number of colloids at each altitude z. Note that adsorption of the colloids on the bottom surface was found to bias the density profiles close to the bottom surface and we thus discarded data from the two first slices. The results of these "Jean-Perrin" experiments are presented in Fig. 3. We have checked that a *stationary* state of the sedimentation profile is reached. As shown in Fig. 3, the density profiles of the active colloidal suspension $\rho(z)$ is decreasing with the altitude z and, as in the thermal case, can be very well fitted by an exponential decay $\rho(z) = \rho_0 \exp(-z/\delta_{\rm eff})$, where ρ_0 was used to normalize the different measurements. The sedimentation length $\delta_{\rm eff}$ is found however to depend strongly on the activity of the colloids: $\delta_{\rm eff}$ increases with an increased propulsion of the colloids, *i.e.* injected energy, as measured (independently) by their effective diffusion coefficient $D_{\rm eff}$. The exponential decay suggests that in the present limit of a dilute active suspension, the active colloids still obey an effective Smoluchowsky equation, with the current replaced by $J = -D_{\rm eff} \nabla \rho + \mu\, mg\, \rho$. This predicts a sedimentation length in the form

$$\delta_{\rm eff} = \frac{1}{v_T} \times D_{\rm eff}, \qquad (2)$$

where $v_T = \mu\, mg$ is the sedimentation velocity in the gravity field.

We have checked this relationship by plotting the sedimentation length measured from the colloid density profiles, against the effective diffusion coefficient measured in the individual tracking measurements. As shown in Fig. 4, the predicted proportionnality between sedimentation length and effective diffuson coefficient is demonstrated experimentally for all propelling activities, with a proportionality constant which is furthermore found to agree with its expected value in Eq. (2). This effectively connects the micro-dynamics of the active colloids to their global stationary profile.

Finally, we have also measured in the previous experiments the mean squared number of particles, ΔN^2(z) in each slice δz for various altitudes z. We plot in Fig. 4-(inset) ΔN^2(z) versus the averaged number $N(z)$ for all fuel concentrations. Data are found to collapse onto a single curve $\Delta N^2 = \kappa \cdot N$ with $\kappa = 1$. This shows that under the present dilute conditions, the active suspension behaves like an equilibrium (ideal) solution, and do not exhibit anomalously large fluctuations ($\Delta N^2 \sim N^\gamma$, with $\gamma > 1$), as previously predicted [1], however for denser ac-

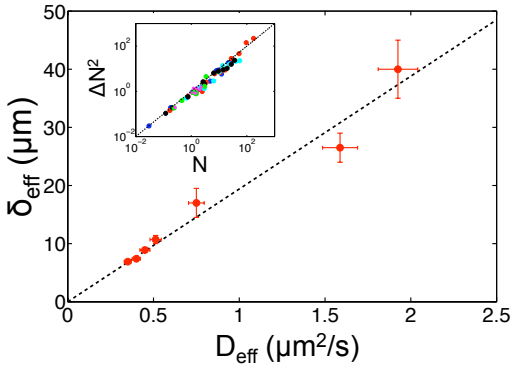

FIG. 4: Sedimentation length $\delta_{\rm eff}$ as a function of effective diffusion $D_{\rm eff}$ extracted from Figs. 2 and 3 respectively. The dashed line is a linear fit, $\delta_{\rm eff} = \alpha \times D_{\rm eff}$ as expected from Eq. (2). The measured slope α =19.5 $\pm$2 μm^{-1}.s is furthermore in good agreement with the expected value $\alpha = 1/v_T = \delta_0/D_0 = 16.2 \pm 2.5$ μm^{-1}.s, with δ_0 and D_0 measured independently in the absence of injected H_2O_2. *Inset:* mean squared number of colloids in each slice ΔN^2 versus the averaged number N for various swimming activity. Symbols are similar to Fig.3. The dashed line is the prediction for equilibrium system $\Delta N^2 = \kappa \cdot N$, with $\kappa = 1$ for dilute systems.

tive systems.

Our results show that in the present regime, the active colloids behave merely as "hot" colloids, with an effective temperature $k_B T_{\rm eff} = D_{\rm eff}/\mu$ much larger than the bare temperature, and do obey an effective Smoluchowsky equation. In the '*run and tumble*' model of particles under external fields discussed by Tailleur and Cates, this behavior is expected in the regime where the swim speed V is larger than the sedimentation velocity v_T. Here $V \sim \mu$m/s, while $v_T = 1/\alpha \sim 50.10^{-3} \mu$m/s – see Fig. 4– , and one has $V/v_T \gg 1$ in the present experiments. Our experimental results thus validate the theoretical expectations in this regime.

To conclude, we have proposed efficient experimental tools allowing to explore the properties of *active colloidal suspensions* under controlled and tunable conditions. This involves artificial chemically active colloids, studied in a dedicated gel microfluidic system. This opens up many perspectives towards a thorough exploration of the out-of-equilibrium behavior of active supensions, in particular for higher volume fractions, where exotic behavior was predicted theoretically, but not observed up to now with artificial active fluids. This involves collective effects, the emergence of flow order, anomalous fluctuations [1], nematic ordering [7], etc. But beyond these predicted behaviors, it is interesting to note that the present colloids not only interact via hydrodynamic flows, but also via *chemical* interactions, through the spatial (diffusive) extension of the consummed fuel. This is expected to affect the many-body behavior of the suspension, with couplings which have not been considered up to now in the litterature. Work along these lines is in progress.

We thank E. Vigier, H. Féret, A. Piednoir, J. Grégoire, J.-M. Benoît. We acknowledge support from Région Rhône-Alpes under program CIBLE.

[1] R.A. Simha, S. Ramaswamy, *Phys. Rev. Lett.* **89**, 058101 (2002).
[2] T. Vicsek, A. Czirók, E. Ben-Jacob, I. Cohen, and O. Shochet. *Phys. Rev. Lett.* **75**, 1226 (1995).
[3] K. Kruse, J. F. Joanny, F. Jülicher, J. Prost, and K. Sekimoto, *Eur. Phys. J. E* **16**, 5 (2005).
[4] I. Llopis and I. Pagonabarraga. *Europhys. Lett.* **75**, 999 (2006).
[5] H. Chaté, F. Ginelli and R. Montagne, *Phys. Rev. Lett.* **96** 180602 (2006).
[6] L. Angelani, R. Di Leonardo, and G. Ruocco, *Phys. Rev. Lett.* **102** 048104 (2009).
[7] A. Baskaran and M.C. Marchetti, *Phys. Rev. Lett.* **101**, 268101 (2008)
[8] J. Tailleur and M.E. Cates *Europhys. Lett.* **86**, 60002, 2009.
[9] E. Lauga and T.R. Powers, *Rep. Prog. Phys.* **72** 096601 (2009)
[10] A.P. Berke, L. Turner, H.C. Berg, E. Lauga, *Phys. Rev. Lett.* **101** 038102 (2008).
[11] K. C. Leptos, J. S. Guasto, J. P. Gollub, A. I. Pesci, and R. E. Goldstein. *Phys. Rev. Lett.* **103** 198103 (2009).
[12] X.-L. Wu and A. Libchaber. *Phys. Rev. Lett.* **84**, 3017 (2000).
[13] L. Cisneros, R. Cortez, C. Dombrowski, R. Goldstein, and J. Kessler. *Exp. Fluids*, **43** 737, 2007.
[14] S. Rafaï, L. Jibuti, P. Peyla, *Phys. Rev. Lett.* **104**, 098102 (2010)
[15] J. R. Howse, *et al. Phys. Rev. Lett.* **99**, 048102 (2007).
[16] R. Dreyfus, *et al. Nature* **437** 862 (2005)
[17] W.F. Paxton *et al. J. Am. Chem. Soc.***26**, 13424 (2004)
[18] R. Golestanian, T.B. Liverpool, A. Ajdari, *Phys. Rev. Lett.* **94**, 220801 (2005)
[19] A. Ajdari and L. Bocquet, *Phys. Rev. Lett.* **96**, 186102 (2006).
[20] B. Abécassis, C. Cottin-Bizonne, C. Ybert, A. Ajdari, L. Bocquet, *Nature Mat.* **7** 785 (2008).
[21] J. Perrin. *Ann. Chim. Phys.* (Paris), **8**, 1 (1909).
[22] J. Diao, *et al. Lab on a Chip*, **6**, 381 (2006).
[23] J. Palacci, B. Abécassis, C. Cottin-Bizonne, C. Ybert, L. Bocquet, *Phys. Rev. Lett.* **104** 138302 (2010).
[24] F. Hediger S.M. Gasser M. Unser D. Sage, F.R. Neumann, *IEEE Transactions on Image Processing*, **14**, 1372, (2005).
[25] M. Born and E. Wolf, *Principle of optics* (Cambridge University Press, 7$^{\rm th}$ Ed., 1999)